Commun Nonlinear Sci Numer Simulat 16 (2011) 133–143

Contents lists available at ScienceDirect

Commun Nonlinear Sci Numer Simulat

journal homepage: www.elsevier.com/locate/cnsns

Suppression of chaotic behavior in horizontal platform systems based on an adaptive sliding mode control scheme

Neng-Sheng Pai, Her-Terng Yau *

Department of Electrical Engineering, National Chin-Yi University of Technology, Taichung 411, Taiwan, ROC

ARTICLE INFO

Article history:
Received 27 December 2009
Received in revised form 15 March 2010
Accepted 13 April 2010
Available online 21 April 2010

Keywords:
Chaos
Horizontal platform
Adaptive sliding mode control
Parametric uncertainties

ABSTRACT

This work presents an adaptive sliding mode control scheme to elucidate the robust chaos suppression control of non-autonomous chaotic systems. The proposed control scheme utilizes extended systems to ensure that continuous control input is obtained in order to avoid chattering phenomenon as frequently in conventional sliding mode control systems. A switching surface is adopted to ensure the relative ease in stabilizing the extended error dynamics in the sliding mode. An adaptive sliding mode controller (ASMC) is then derived to guarantee the occurrence of the sliding motion, even when the chaotic horizontal platform system (HPS) is undergoing parametric uncertainties. Based on Lyapunov stability theorem, control laws are derived. In addition to guaranteeing that uncertain horizontal platform chaotic systems can be stabilized to a steady state, the proposed control scheme ensures asymptotically tracking of any desired trajectory. Furthermore, the numerical simulations verify the accuracy of the proposed control scheme, which is applicable to another chaotic system based on the same design scheme.

1. Introduction

Chaos dynamics has received considerable attention in the recent decade owing to the promising attributes of chaotic systems such as highly complex dynamics, broad-band Fourier power spectrum, sensitivity to initial conditions and strange attractors [1,2]. Many theoretical and experimental chaos analyses-based methods have subsequently been thoroughly investigated [3]. Moreover, several mechanical systems with chaotic phenomena have also been developed in recent years [4,5]. Horizontal platform, i.e. a mechanical system with chaos behavior that can freely rotate around the horizontal axis, has been extensively adopted in offshore and earthquake engineering [6].

Recently, a study on chaos control investigated its role in autonomous chaotic systems such as Chua's circuit, Lorenz system and Chen system [7]. An increasing number of non-autonomous chaotic systems have been developed in engineering and physics, motivating the study of chaos control for various non-autonomous systems. In 2003, Ge et al. [8] studied a chaos synchronization scheme consisting two non-autonomous horizontal platform systems that are unidirectionally coupled by linear state error feedback control. Their numerical results verified that the scheme can achieve chaos synchronization regardless of whether a phase mismatch occurs between two coupled systems, provided that the coupling strength is sufficiently large. Wu et al. [9,10] later studied the robust synchronization of chaotic horizontal platform systems with phase difference. However, as is known, if horizontal platform systems operate in a state of aperiodic motion, the subsequently large broad-band vibration may increase the likelihood of fatigue failure and shorten the system lifetime. Therefore, designing a controller to suppress the chaotic behavior in the horizontal platform systems is also a very important problem. However, suppressing the chaotic behavior of horizontal platform systems has seldom been studied.

* Corresponding author. Tel.: +886 423924505x7229; fax: +886 423930062.
E-mail addresses: pan1012@ms52.hinet.net, htyau@ncut.edu.tw (H.-T. Yau).

1007-5704/$ - see front matter © 2010 Elsevier B.V. All rights reserved.
doi:10.1016/j.cnsns.2010.04.014

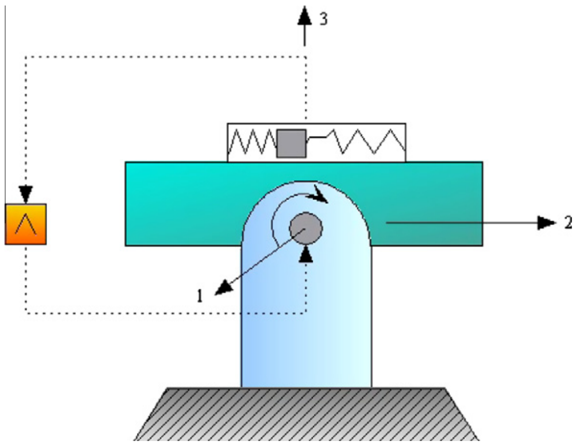

Fig. 1. Horizontal platform system.

This work presents an adaptive sliding mode control scheme for controlling the chaos in the state trajectories of uncertain horizontal platform systems. The proposed control scheme utilizes extended systems to ensure that continuous control input is obtained in order to prevent chattering that occurs frequently in conventional sliding mode control systems. A switching surface is adopted to ensure the stability of the extended error dynamics in the sliding mode. Based on this switching surface, a continuous adaptive sliding mode control (SMC) is derived not only to guarantee the sliding motion, but also to avoid the chattering, even when the system is undergoing unknown system uncertainty. The proposed sliding mode controller scheme can effectively suppress the chaotic behavior in horizontal platform systems even if parametric uncertainty occurs. The rest of this paper is organized as follows. Section 2 describes the dynamics of horizontal platform systems. Section 3 then introduces the design scheme of the switching surface and sliding mode controller. Next, Section 4 summarizes the simulation results to demonstrate the effectiveness of the proposed adaptive control scheme for chaos control of horizontal platform systems. Conclusions are finally drawn in Section 5, along with recommendations for future research. Notably, $\lambda_i(A)$ denotes the ith eigenvalue of the matrix A, $\lambda_{\max}(A) = \max_i Re(\lambda_i(A))$ represents the eigenvalue of matrix A with maximum real part and $|w|$ is the absolute value of w. Meanwhile, for $w \in R^n$, $\|w\| = \sqrt{(w^T w)}$ denotes the Euclidean norm and sign(s) represents the sign function of s, if, sign(s) = 1; if $s = 0$, sign(s) = 0; if $s < 0$, sign(s) = -1.

2. Mathematical modelling

Figs. 1 and 2 show the nonlinear dynamics of horizontal platform system (HPS). The platform can freely rotate around the horizontal axis, which penetrates its mass center. An accelerometer is located on the platform to detect the position. The accelerometer produces an output signal to the actuator, subsequently generating a torque to inverse the rotation of the platform to balance the HPS, when the platform deviates from horizon. The dynamics can be described as

$$A\ddot{x}(t) + D\dot{x}(t) + rg\sin x(t) - \frac{3g}{R}(B - C)\cos x(t)\cdot\sin x(t) = F\cos\omega t \tag{1}$$

where A, B and C are the inertia moment of the platform for axis 1, 2 and 3, respectively. Additionally, D denotes the damping coefficient. R represents the radius of the earth, r is the proportional constant of the accelerometer, g denotes the constant of gravity, x represents the rotation of the platform in relation to the earth and $F\cos wt$ is the harmonic torque. A more detailed analysis of this system can be found in [8]. By denoting $x_1(t) = x(t)$ and $x_2(t) = \dot{x}(t)$ as the state variables and defining parameters $a = D,\ rg = b,\ l = \frac{3g}{R}(B - C)$ and $F = h$, the HPS model (1) can be rewritten as follows:

$$\begin{aligned} \dot{x}_1 &= x_2 \\ \dot{x}_2 &= -ax_2 - b\sin x_1 + l\cos x_1\cdot\sin x_1 + h\cos\omega t \end{aligned} \tag{2}$$

Parameters of the horizontal platform systems are taken as $a = 4/3$, $b = 3.776$, $l = 4.6\times10^{-6}$, $h = 34/3$ and $\omega = 1.8$. As the preliminary states $(x_1(0),x_2(0)) = (-3.4,2.1)$, the trajectory of HPS is chaotic [10]. The trajectories display randomly and remarkably in the course of time (Fig. 3).

3. Controller design for uncertain HPS

3.1. Error dynamics of HPS

The chaotic behavior in HPS is suppressed by adding a control input u in Eq. (2). Therefore, the controlled HPS is shown as follows:

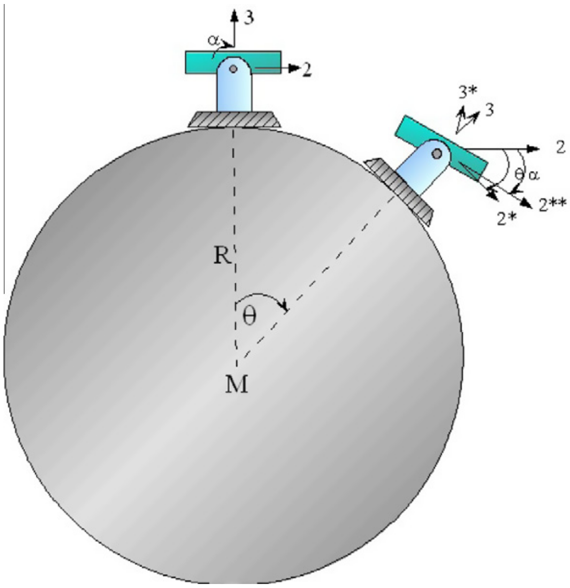

Fig. 2. Horizontal platform system on the earth.

$$\begin{aligned}\dot{x}_1 &= x_2 \\ \dot{x}_2 &= -(a+\Delta a)x_2 - (b+\Delta b)\sin x_1 + l\cos x_1 \cdot \sin x_1 + h\cos\omega t + u\end{aligned} \tag{3}$$

where Δa and Δb denote the parametric uncertainties of HPS. Notably, Δa and Δb are assumed here to be bounded, i.e.

$$|\Delta a| \leqslant \alpha \quad \text{and} \quad |\Delta b| \leqslant \beta \tag{4}$$

where α and β are positive constants. The control problem manipulates the system to track the desired regular angle trajectories x_d (i.e. x_d is a differential function). By allowing the tracking error to be $E(t) = (x_1 - x_d, x_2 - \dot{x}_d) = (e_1, e_2)$, the error dynamics becomes

$$\begin{aligned}\dot{e}_1 &= e_2 \\ \dot{e}_2 &= f(t) + \xi(t) + u(t)\end{aligned} \tag{5}$$

where

$$f(t) = -a(e_2 + \dot{x}_d) - b\sin(e_1 + x_d) + l\cos(e_1 + x_d)\cdot\sin(e_1 + x_d) + h\cos\omega t \tag{6}$$

and

$$\xi(t) = -\Delta a(e_2 + \dot{x}_d) - \Delta b\sin(e_1 + x_d) \tag{7}$$

Therefore, for any given chaotic uncertain HPS, e.g., (3), this work designs an adaptive sliding mode controller (ASMC), so that, the asymptotic stability of the resulting error system (5) can be achieved in the sense that

$$\|E(t)\| = \|[e_1 \;\; e_2]\| \to 0 \quad \text{as} \;\; t \to \infty,$$

where $\|\cdot\|$ is the Euclidean norm of a vector.

The following assumption is made to derive the main results.

Assumption 1. For the nonlinear function $f(t)$ of (6) and the uncertainty term $\xi(t)$ of (7), a sufficiently large constant ρ satisfies

$$\left|\frac{d}{dt}[f(t) + \xi(t)]\right| \leqslant \rho < \infty \tag{8}$$

Remark 1. Notably, the unknown but constant ρ is only introduced to verify the stability later; the value of ρ for the control design does not need to be known. Thus, ρ is assumed here to be sufficiently large, i.e. $\rho \to \infty$, so the assumption of (8) always holds.

Introducing the concept of extended systems [11], the error dynamics in (6) can be extended as

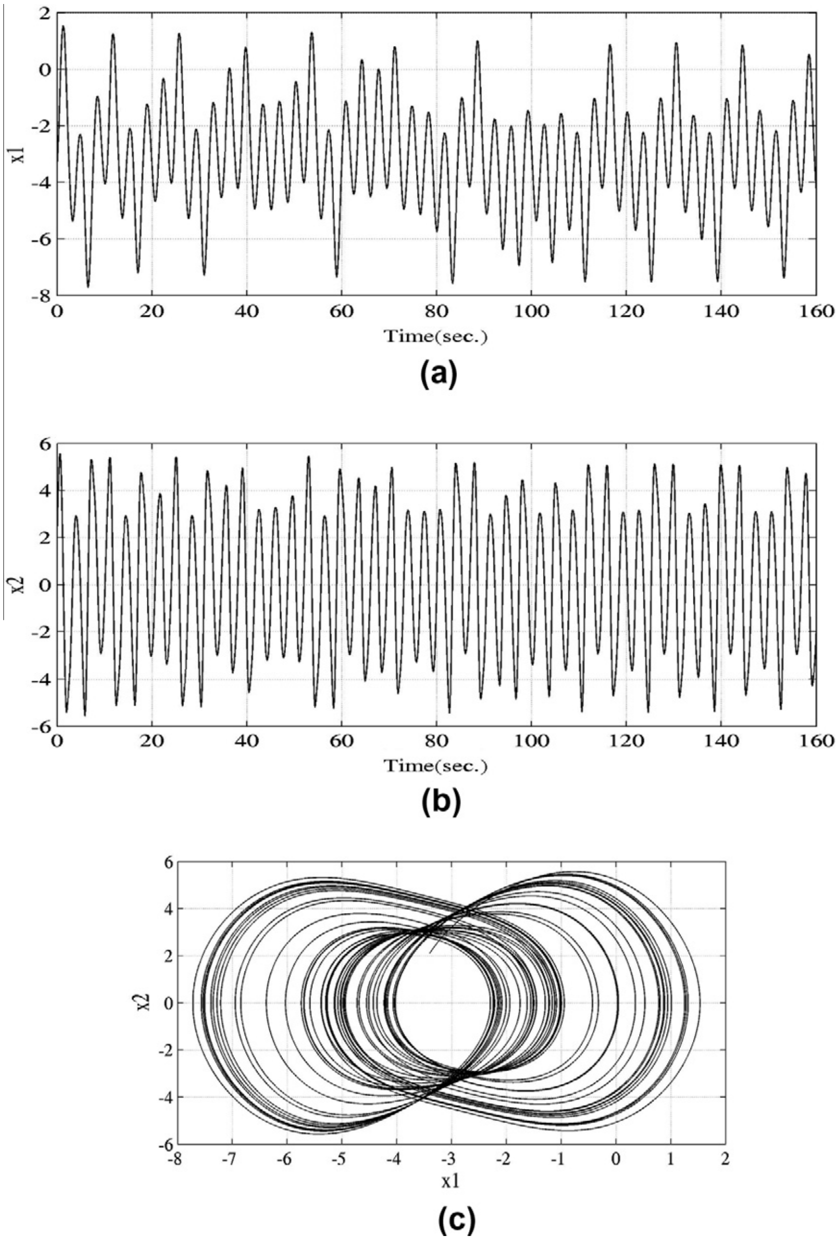

Fig. 3. The chaotic response of the HPS.

$$
\begin{aligned}
\dot{e}_1 &= e_2 \\
\dot{e}_2 &= f(t) + \xi(t) + u = e_3 \\
\dot{e}_3 &= \frac{d}{dt}[f(t) + \xi(t)] + \dot{u}
\end{aligned} \tag{9}
$$

System (9) is of the controllable canonical form. In such a case, no internal dynamics occur.

3.2. Sliding surface design

Implementing the sliding mode control (SMC) scheme to control a chaotic system generally involves two steps. An appropriate switching surface must be selected first, capable of ensuring the stability of the equivalent dynamics in the sliding mode such that the error dynamics (5) can converge to zero. A SMC must then be determined to ensure not only the striking of the switching surfaces in finite time, but also that the state trajectory can remain on the sliding mode $s = 0$ thereafter even when undergoing the system uncertainties. As mentioned earlier, a proper switching surface must be designed to ensure the system stability in the sliding mode. The asymptotical stability of the sliding mode can be ensured by defining a switching surface $s(t)$ in the extended error space as follows:

$$s(t) = e_3(t) + k_2 e_2(t) + k_1 e_1(t) \tag{10}$$

where $s(t) \in R$ and k_1,k_2 are that design parameters that can be easily determined later. A system that operates in the sliding mode satisfies the following equations [11,12]:

$$s(t) = 0 \tag{11}$$

Therefore, the following sliding mode dynamics can be obtained as:

$$\begin{bmatrix} \dot{e}_1 \\ \dot{e}_2 \end{bmatrix} = \begin{bmatrix} 0 & 1 \\ -k_1 & -k_2 \end{bmatrix} \begin{bmatrix} e_1 \\ e_2 \end{bmatrix} = A \begin{bmatrix} e_1 \\ e_2 \end{bmatrix} \tag{12.a}$$

$$\dot{e}_3 = \frac{d}{dt}[f(t) + \xi(t)] + \dot{u} \tag{12.b}$$

Obviously, if the design parameters k_1, k_2 are specified to ensure $\lambda_{\max}(A) < 0$, the stability of (12.a) is guaranteed, i.e. $\lim_{t\to\infty}\|[e_1 \ e_2]\| = 0$. Furthermore, according to Eq. (11), $e_3(t)$ is also stable, that is $\lim_{t\to\infty} e_3(t) = 0$.

3.3. Sliding mode controller design

With an appropriate switching surface established, the next step involves designing an adaptive SMC scheme to drive the extended error system trajectories onto the switching surface $s(t) = 0$. Before the adaptive SMC design is introduced, the Barbalat lemma is given below.

Lemma 1 (Barbalat lemma, [12]). *If $F{:}R \to R$ is a uniformly continuous function for $t \geqslant 0$ and if the limit of the integral*

$$\lim_{t\to\infty} \int_0^t |F(\lambda)|\, d\lambda \tag{13}$$

exists and is finite, then

$$\lim_{t\to\infty} F(t) = 0 \tag{14}$$

To ensure the occurrence of the sliding motion, an adaptive scheme is proposed as

$$\dot{u}(t) = -k_1 e_2(t) - k_2 e_3(t) - \gamma \hat{\kappa}(t) \operatorname{sign}(s(t)), \qquad u(0) = u_0 \tag{15}$$

where $\gamma > 1$ and u_0 is the bounded initial value of $u(t)$. The adaptive law is

$$\dot{\hat{\kappa}}(t) = q|s(t)|; \qquad \hat{\kappa}(0) = \hat{\kappa}_0 \tag{16}$$

where the parameter q of adaptive law is selected as positive value and $\hat{\kappa}_0$ denotes the bounded initial value of $\hat{\kappa}(t)$. The adaptive SMC controller can be also written in the following integral form:

$$u(t) = \int_0^t [-k_1 e_2(t) - k_2 e_3(t) - \gamma \hat{\kappa}(t) \cdot \operatorname{sign}(s)]\, dt + u_0 \tag{17}$$

and

$$\hat{\kappa}(t) = q \int_0^t |s(t)|\, dt + \hat{\kappa}_0 \tag{18}$$

Remark 2. In the conventionally adopted SMC controller, the control scheme is often discontinuous, causing chattering in the sliding mode. However, the proposed adaptive controller scheme as shown in (17) is continuous. Therefore, chattering in the sliding mode is eliminated.

Remark 3. From Eqs. (15)–(18), it seen that the values of parameter q and $\hat{\kappa}_0$ can influence $\hat{\kappa}(t)$. Furthermore, the value of $\hat{\kappa}(t)$ dominate the hitting time of sliding surface. We can obtain a shorter hitting time if we increase the positive value of $\hat{\kappa}(t)$. However, a larger value of $\hat{\kappa}(t)$ will cause a larger value of control input. It may lead to the phenomenon of saturation. Therefore, we can obtain the suitable values of q and $\hat{\kappa}_0$ by trial and error method.

Next, the proposed adaptive SMC (17) is demonstrated to be capable of driving the extended error dynamics (9) onto the sliding mode $s(t) = 0$.

3.4. Robust stability analysis

The following discussion establishes that if the control input $u(t)$ is appropriately designed as (15) with adaption law (16), then the trajectory of the error dynamics (9) converges to the switching surface $s(t) = 0$. Consider the following Lyapunov function candidate:

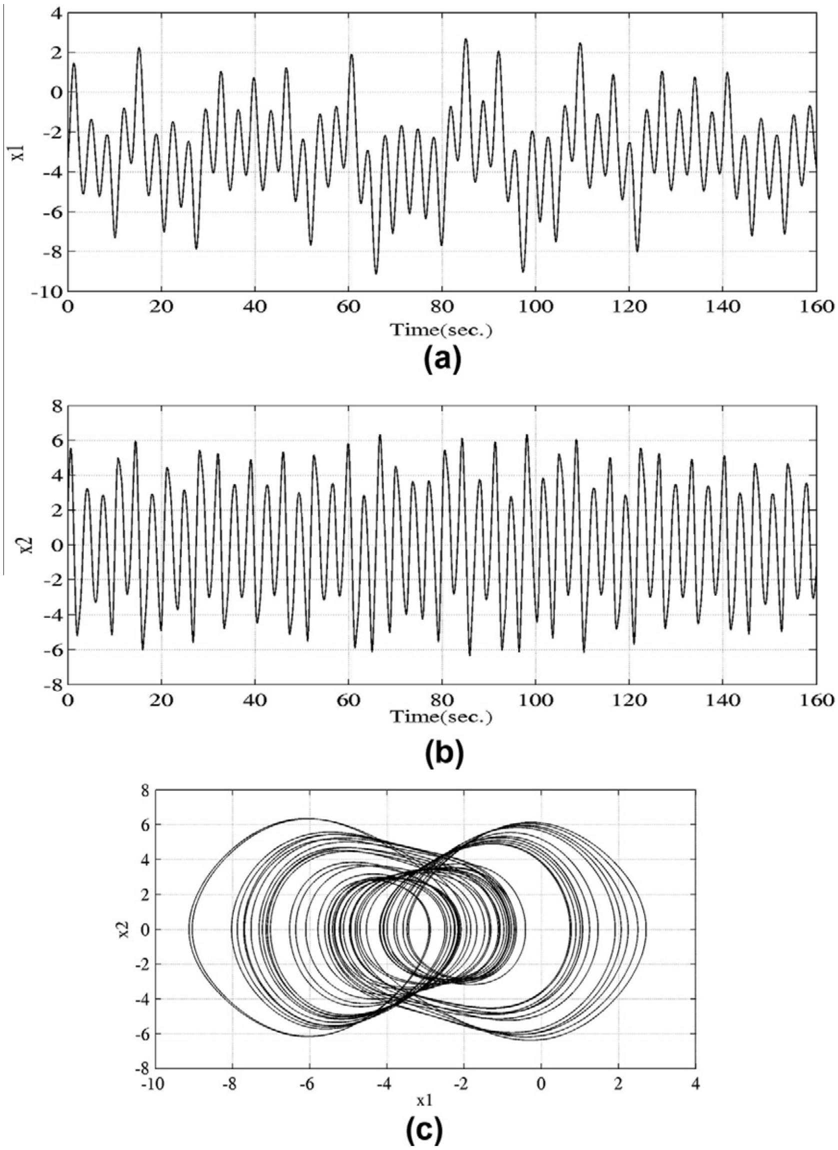

Fig. 4. The chaotic response of the uncertain HPS.

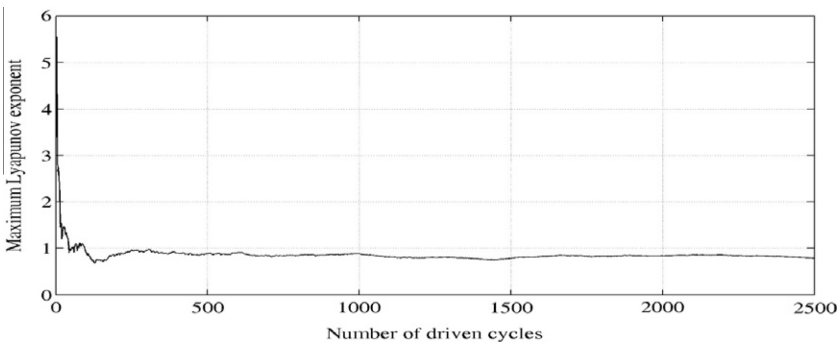

Fig. 5. Maximum Lyapunov exponent of uncertain HPS trajectory plotted as function of number of driven cycles.

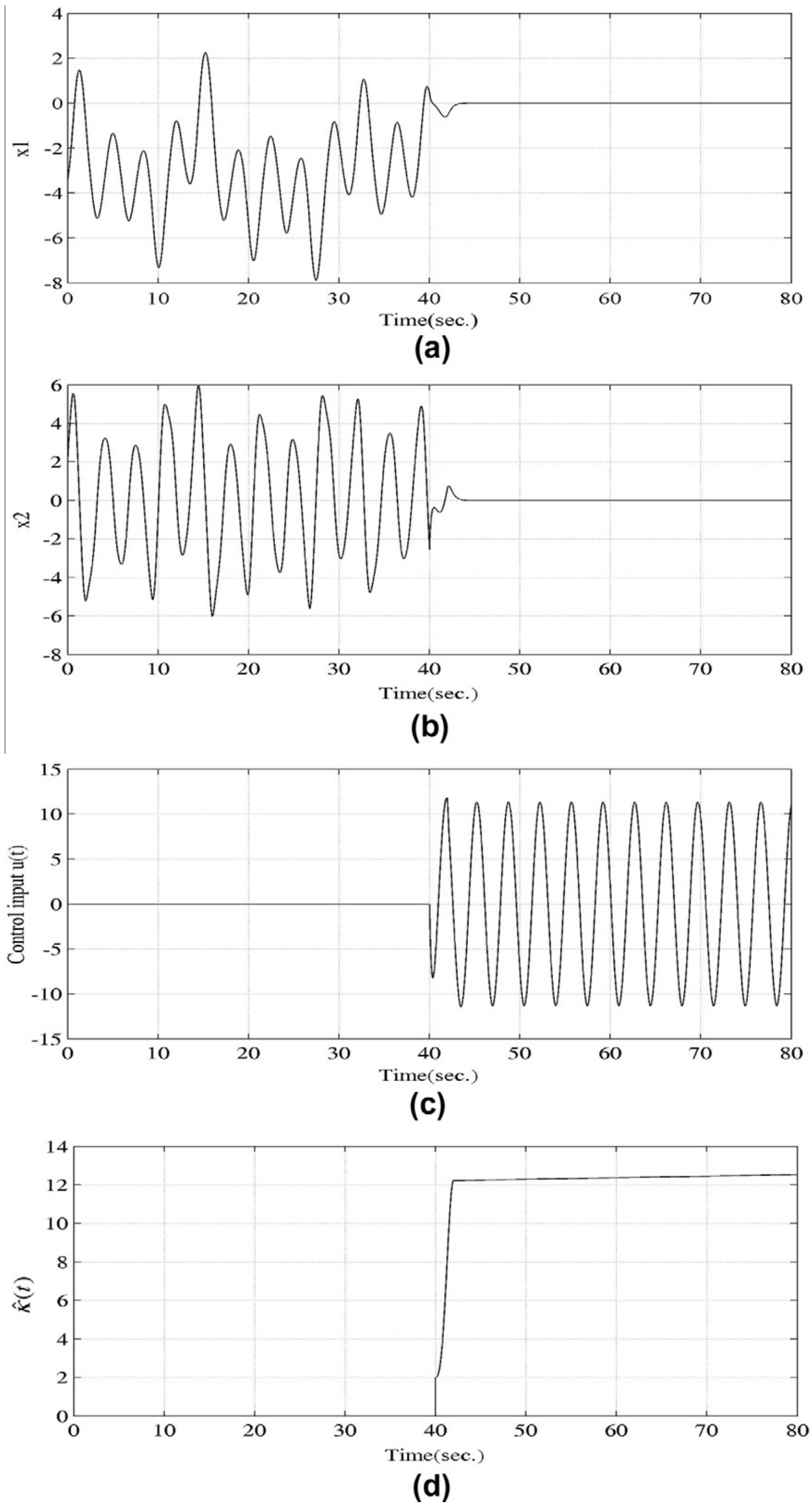

Fig. 6. The time history of controlled system for $x_d = 0$; (a) time response of x_1; (b) time response of x_2; (c) time response of control input; (d) time response of adaptation parameter $\hat{\kappa}(t)$; and (e) time response of sliding surface. The control u is activated at $t = 40$ s.

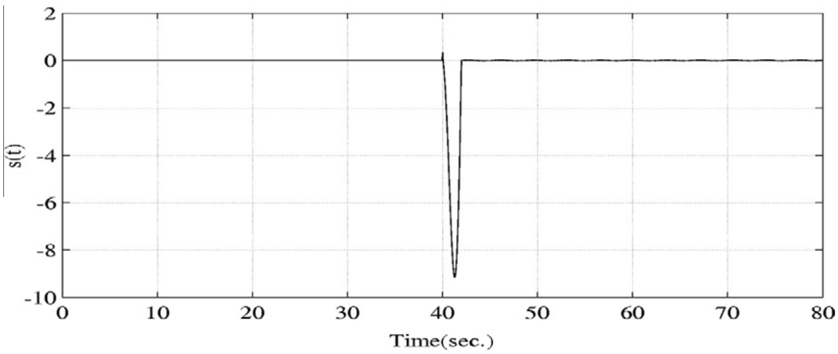

Fig. 6 (*continued*)

$$V(t) = \frac{1}{2}(s^2 + q^{-1}\delta^2); \qquad q > 0 \tag{19}$$

where $\delta \in R$ denotes the adaptation error defined later. Taking the derivative of $V(t)$ with respect to time yields

$$\dot{V}(t) = s\dot{s} + q^{-1}\delta\dot{\delta} = s(\dot{e}_3 + k_2 e_3 + k_1 e_2) + q^{-1}\delta\dot{\delta} = s\left[\frac{d}{dt}(f(t) + \xi(t)) + k_2 e_3 + k_1 e_2 + \dot{u}\right] + q^{-1}\delta\dot{\delta} \tag{20}$$

Now let $\delta = \rho - \hat{\kappa}(t)$ denote the adaptation error. Since ρ is constant, $\dot{\rho} = 0$ and the following expression holds:

$$\dot{\delta} = -\dot{\hat{\kappa}}(t) \tag{21}$$

Then, Eq. (20) can be rewritten as

$$\dot{V}(t) = s\left[\frac{d}{dt}(f(t) + \xi(t)) + k_2 e_3 + k_1 e_2 + \dot{u}\right] - q^{-1}\left(\rho - \hat{k}\right)\dot{\hat{k}} \tag{22}$$

Substituting $\dot{u}$ and $\dot{\hat{k}}$ into the above equation yields

$$\begin{aligned} \dot{V}(t) &= s\left[\frac{d}{dt}(f(t) + \xi(t)) - \gamma \cdot \hat{k} \cdot \mathrm{sign}(s)\right] - \left(\rho - \hat{k}\right)|s| = s\left[\frac{d}{dt}(f(t) + \xi(t))\right] - \rho|s| + (1-\gamma)\hat{k}|s| \\ &\leqslant |s|\left|\frac{d}{dt}(f(t) + \xi(t))\right| - \rho|s| + (1-\gamma)\hat{k}|s| \leqslant (1-\gamma)\hat{k}|s| \leqslant -F(t) \end{aligned} \tag{23}$$

where $F(t) = (\gamma - 1)\hat{k}(t)|s(t)| \geqslant 0$ and $\gamma > 1$.

Integrating the above equation from zero to t yields

$$V(0) \geqslant V(t) + \int_0^t F(\lambda)\,d\lambda \geqslant \int_0^t F(\lambda)\,d\lambda \tag{24}$$

As t goes infinite, the above integral is always less than or equal to $V(0)$. Since $V(0)$ is positive and finite, $\lim_{t\to\infty}\int_0^t F(\lambda)\,d\lambda$ exists and is finite. Thus, according to Barbalat lemma (see Lemma 1), we obtain

$$\lim_{t\to\infty} F(t) = \lim_{t\to\infty}(\gamma - 1)\hat{\kappa}(t)|s| = 0 \tag{25}$$

Since both $(\gamma - 1)$ and $\hat{\kappa}(t)$ are greater than zero, (25) implies $s = 0$. Hence, the proof is achieved.

4. Results and discussion

This section presents the simulation results to demonstrate the performance of the proposed controller scheme. The parameters are $a = 4/3$, $b = 3.776$, $l = 4.6 \times 10^{-6}$, $h = 34/3$, $\omega = 1.8$. The initial state is $(x_1(0), x_2(0)) = (-3.4, 2.1)$. The parametric uncertainties Δa and Δb are assumed to be $\Delta a = 0.1 \cdot \sin(t)$, $\Delta b = 0.2 \cdot \cos(t)$, then $|\Delta a| \leqslant 0.1 = \alpha$, $|\Delta b| \leqslant 0.2 = \beta$. Fig. 4 shows the time responses and phase plane trajectory of uncontrolled HPS ($u = 0$ in system (3)), indicating that the behavior of uncontrolled uncertain HPS is still extremely complex. According to Fig. 5, the corresponding maximum Lyapunov exponent has a positive value. We can thus infer that the uncertain HPS trajectory is in a state of chaotic motion [3]. The controller scheme attempts to suppress this undesired chaotic behavior. As mentioned in Section 3, the proposed design procedure can be obtained as follows:

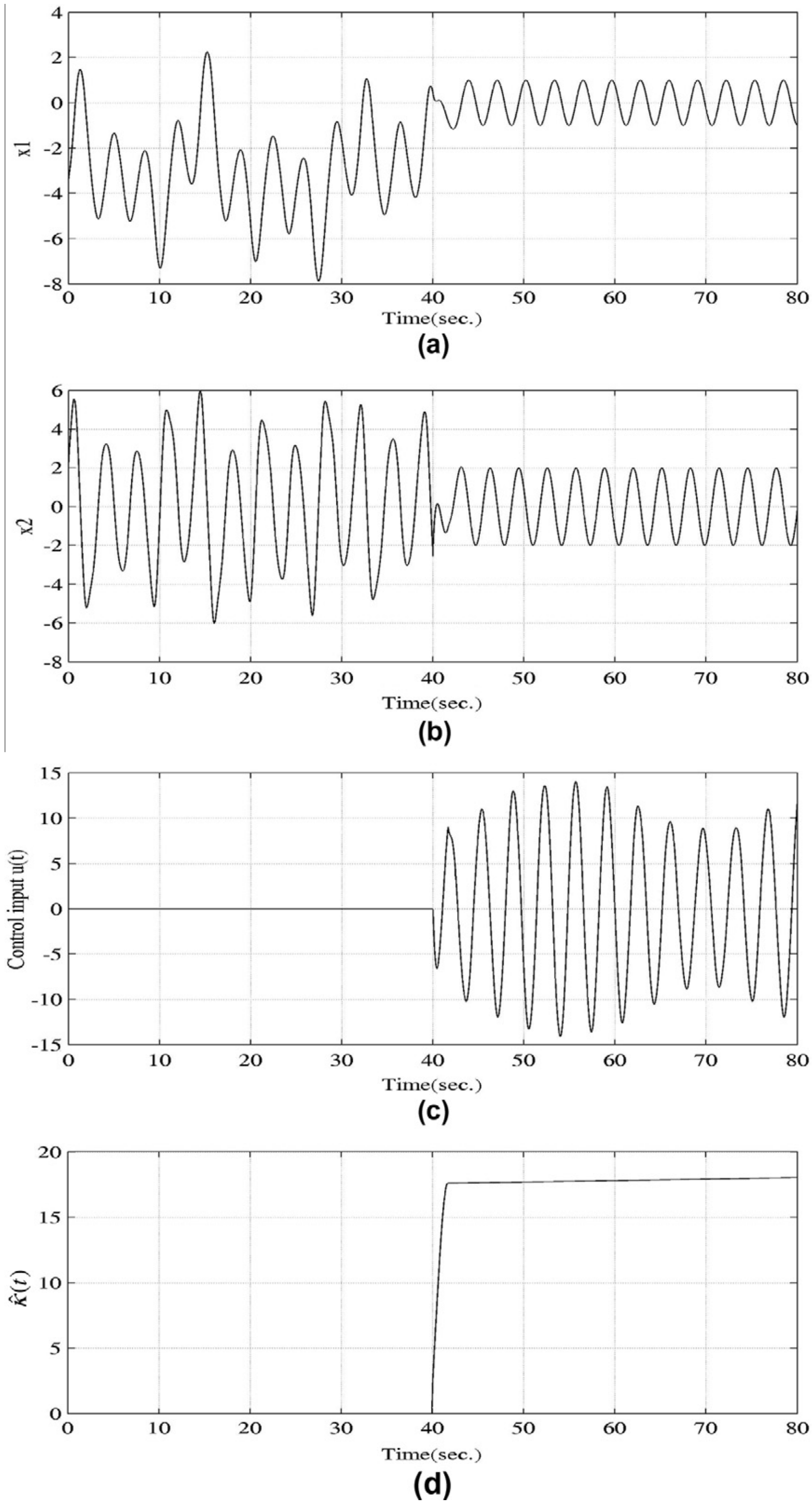

Fig. 7. The time history of controlled system for $x_d = \sin(2t)$; (a) time response of x_1; (b) time response of x_2; (c) time response of control input; (d) time response of adaptation parameter $\hat{\kappa}(t)$; (e) time response of sliding surface; and (f) time response of error dynamics. The control u is activated at $t = 40$ s.

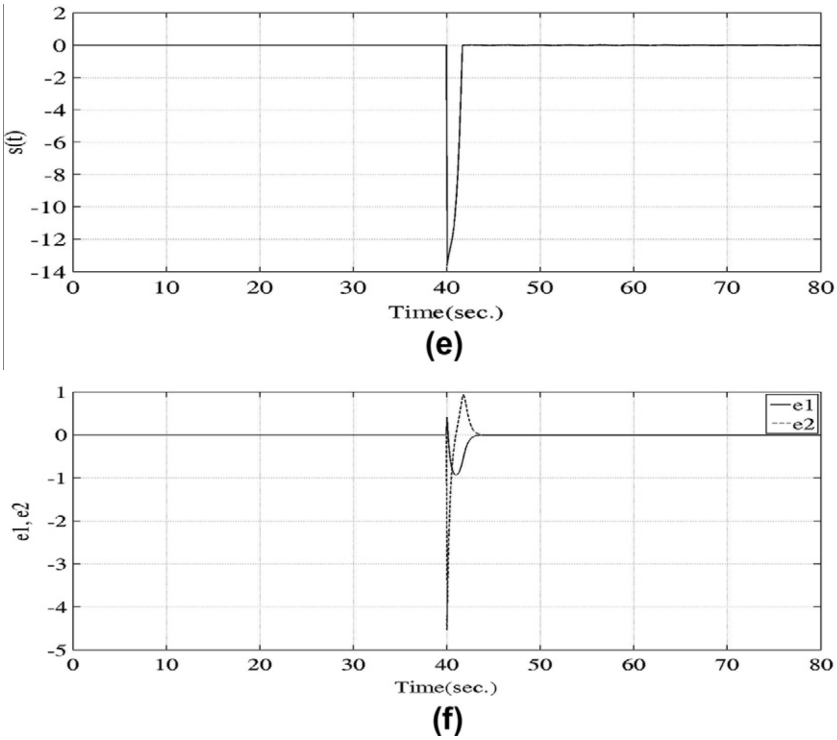

Fig. 7 (*continued*)

Step 1: According to (12.a), select $k_1 = 12$, $k_2 = 7$ such that $\lambda(A) = (-4, -3)$, resulting in a stable sliding mode. Therefore, the switching surface equation is obtained as

$$s(t) = e_3(t) + 7e_2(t) + 12e_1(t) \tag{26}$$

Step 2: From (17) and (18), determine the continuous control input as

$$u(t) = \int_0^t [-12e_2(t) - 7e_3(t) - \gamma\hat{\kappa}(t)\text{sign}(s(t))]dt + u_0 \tag{27}$$

where $\gamma = 1.2 > 1$ and $u_0 = 0$.
The adaptive law is

$$\hat{\kappa}(t) = q\int_0^t |s(t)|\,dt + \hat{\kappa}_0 \tag{28}$$

where $q = 1$ and $\hat{\kappa}_0 = 2$.

Figs. 6 and 7 summarize the simulation results under the proposed adaptive sliding mode controller (27). The first simulation case is $x_d = 0$ (regulation problem). Fig. 6 displays those results, indicating that the system is uncontrolled and the trajectories are chaotic during the first 40 s. The control input is activated at $t = 40$ s. Following the transient response, the chaotic behavior of the uncontrolled system is suppressed to zero. The corresponding control input continues (Fig. 6(c)). According to this figure, chattering does not occur, due to the continuous control. Fig. 6(d) and (e) shows the time responses of corresponding $s(t)$ and adaptation parameter $\hat{\kappa}(t)$. The second simulation case is $x_d = \sin(2t)$ (tracking problem). Fig. 7 summarizes those results. The time responses of controlled system states are tracked to $x_d = \sin(2t)$ after the control becomes active at $t = 40$ s. Fig. 7(c)–(f) shows the continuous control input, time response of sliding surface $s(t)$, adaptation parameter $\hat{\kappa}(t)$ and error state dynamics, indicating that the uncertain chaotic HPS can be steered to a periodic orbit.

5. Conclusion

This work presents an adaptive sliding mode control scheme for suppressing uncertain chaotic behavior in horizontal platform systems. Based on a rigorous mathematical analysis and Lyapunov stability theory, an adaptive sliding mode controller is designed such that the controlled system state can be driven to a desired orbit. Simulation results indicate that the proposed continuous control input can stabilize an uncertain chaotic HPS. Under the proposed control scheme, the error state convergence time can be arbitrarily determined by assigning corresponding eigenvalues of the sliding surfaces. Analysis and simulation results demonstrate that the proposed adaptive sliding mode control is highly promising for suppressing uncertain chaotic dynamics, even for higher-dimensional and complex systems.

References

[1] Bishop SR, Clifford MJ. Zone of chaotic behavior in the parametrically excited pendulum. J Sound Vib 1996;189:142–7.
[2] Chen HK. Chaotic and chaos synchronization of symmetric gyro with linear-plus-cubic damping. J Sound Vib 2002;255:719–40.
[3] Chen G, Dong X. From chaos to order: methodologies, perspectives and applications. Singapore: World Scientific; 1998.
[4] Yau HT. Chaos synchronization of two uncertain chaotic nonlinear gyros using fuzzy sliding mode control. Mech Syst Signal Proces 2008;22:408–18.
[5] Wang CC, Pai NS, Yau HT. Chaos control in AFM system using sliding mode control by backstepping design. Commun Nonlinear Sci Numer Simulat 2010;15(3):741–51.
[6] Huang CL. Nonlinear dynamics of the horizontal platform, Master of Science in Mechanical Engineering Thesis, NCTU; 1996.
[7] Hu J, Chen S, Chen L. Adaptive control for anti-synchronization of Chua's chaotic system. Phys Lett A 2005;339:455–60.
[8] Ge ZM, Yu TC, Chen YS. Chaos synchronization of a horizontal platform system. J Sound Vib 2003;268:731–49.
[9] Wu XF, Cai JP, Wang MH. Master–slave chaos synchronization criteria for the horizontal platform systems via linear state error feedback control. J Sound Vib 2006;295:378–87.
[10] Wu XF, Cai JP, Wang MH. Robust synchronization of chaotic horizontal platform systems with phase difference. J Sound Vib 2007;305:481–91.
[11] Yau HT. Design of adaptive sliding mode controller for chaos synchronization with uncertainties. Chaos Soliton Fract 2004;22(2):341–7.
[12] Slotine JE, Li W. Applied nonlinear control. Englewood Cliffs (NJ): Prentice-Hall; 1991.